

## Electronic Supporting Information

### Synthesis of a Pyridyl-Appended Calix[4]arene and its Application to the Modification of Silver Nanoparticles as an Fe<sup>3+</sup> Colorimetric Sensor

Junyan Zhan, Long Wen, Fajun Miao, Demei Tian and Haibing Li\*

*Key Laboratory of Pesticide and Chemical Biology of Ministry of Education, College of Chemistry,  
Central China Normal University, Wuhan 430079, China Tel: +86-27-67866423  
E-mail: [lhbing@mail.ccnu.edu.cn](mailto:lhbing@mail.ccnu.edu.cn)*

#### Content

The procedure of synthesis of 4-propynoxypyridine

Figure S1. The plot of  $1/I$  versus mole fraction of Fe<sup>3+</sup>

Figure S2. Job's plots of **2** toward Fe<sup>3+</sup>

Figure S3. The MALDI-TOF mass spectrum of the **2**·Fe<sup>3+</sup> complex

Figure S4. Photographs of the fluorescence responses of **2** in the absence and presence of Fe<sup>3+</sup> under UV light

Figure S5. The fluorescence changes of **2** toward Fe<sup>3+</sup> in the presence of other ions.

Figure S6. The partial <sup>1</sup>H NMR spectra of **2** and in the presence of Fe(ClO<sub>4</sub>)<sub>3</sub>

**Figure S7. The optimized structure of the **2**·Fe<sup>3+</sup> complex**

Figure S8. The photographic images, UV-vis spectra and the stability of **2**-Ag NPs

Figure S9. Size distribution of TEM images of **2**-Ag NPs

**Figure S10. FT-IR spectra of calix[4]arene 2 and 2-Ag NPs**

**Figure S11.  $^1\text{H}$  NMR of calix[4]arene 2 and 2-Ag NPs**

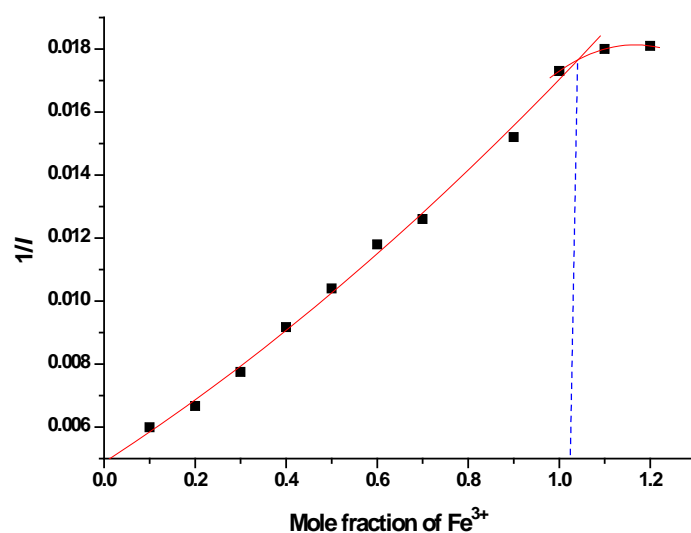
**Figure S12. The UV-vis spectra of 2-Ag NPs, in the presence of alkali metal ions and alkaline earth metal ions**

**Figure S13. The photographic images, UV-vis spectra and the dependence of the R values of 2-Ag NPs on the increasing concentration of  $\text{Fe}^{3+}$**

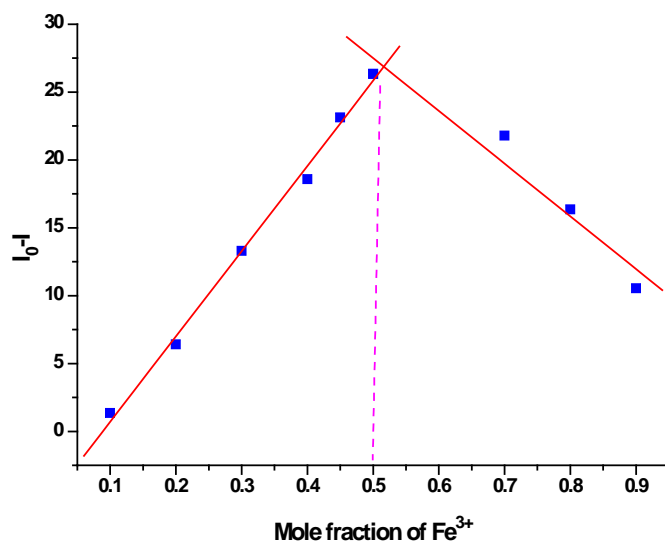
**Figure S14. NMR, HDMS spectra of calix[4]arene 2**

### The procedure of synthesis of 4-propynoxy pyridine

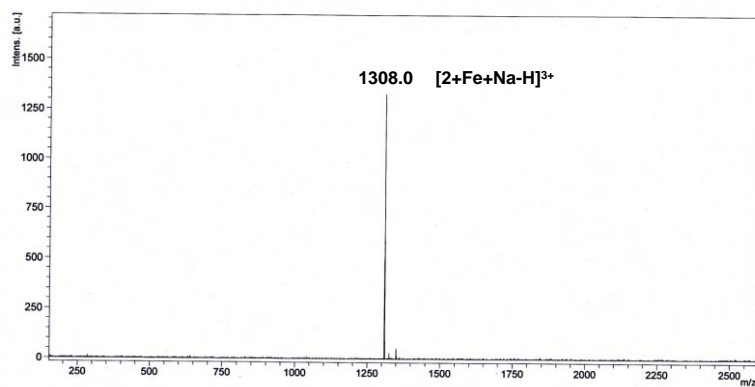
A suspension of 4-hydroxy pyridine (0.57 g, 6 mmol) and anhydrous potassium carbonate (1.66 g, 12 mmol) in acetone (20 mL) was stirred for 0.5 h at room temperature. Then a solution of 3-bromopropyne (1.3 mL, 12 mmol) dissolved in acetone (5 mL) was slowly added. The reaction mixture was stirred for 2 h at 50 °C. The cooled reaction mixture was filtered and washed with acetone. The filtrate were removed under vacuum and the residue was further purified by column chromatography eluting with ethyl acetate/methanol (v/v= 5:1); Yield: 95%. <sup>1</sup>H NMR (600 MHz, CDCl<sub>3</sub>): δ 7.45 (d, *J* = 7.2 Hz, 2H, PyH), 6.42 (d, *J* = 7.2 Hz, 2H, PyH), 4.60 (s, 2H, OCH<sub>2</sub>Py), 2.65 (s, 1H, CCH).



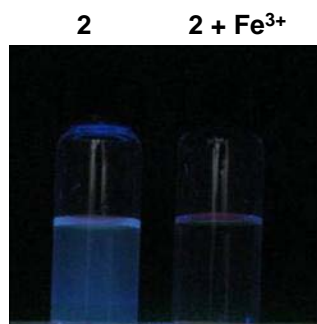
**Fig. S1.** The plot of  $1/I$  versus mole fraction of  $\text{Fe}^{3+}$ . Fluorescence spectra of **2** ( $5 \times 10^{-5}$  M) with various equivalents of  $\text{Fe}^{3+}$  in  $\text{CH}_3\text{CN}$  (0 -1.2 equiv).



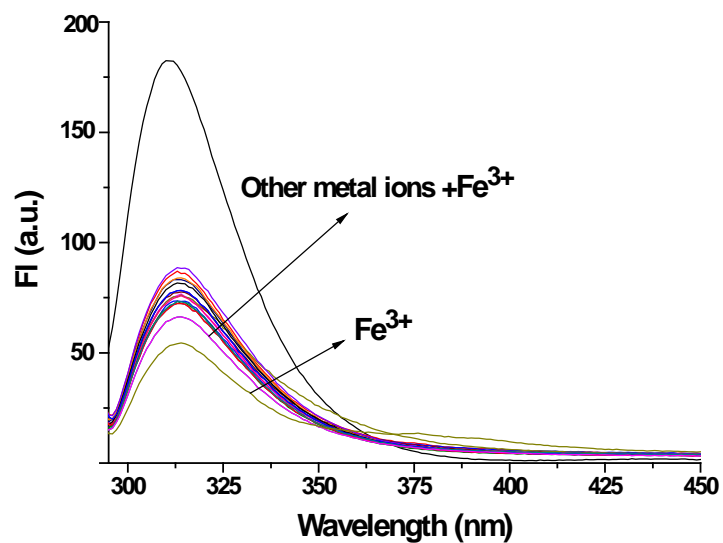
**Fig. S2.** Job's plots of **2** toward Fe<sup>3+</sup> in CH<sub>3</sub>CN solution at an invariant total concentration of 10<sup>-5</sup> M. (Excitation 285nm)



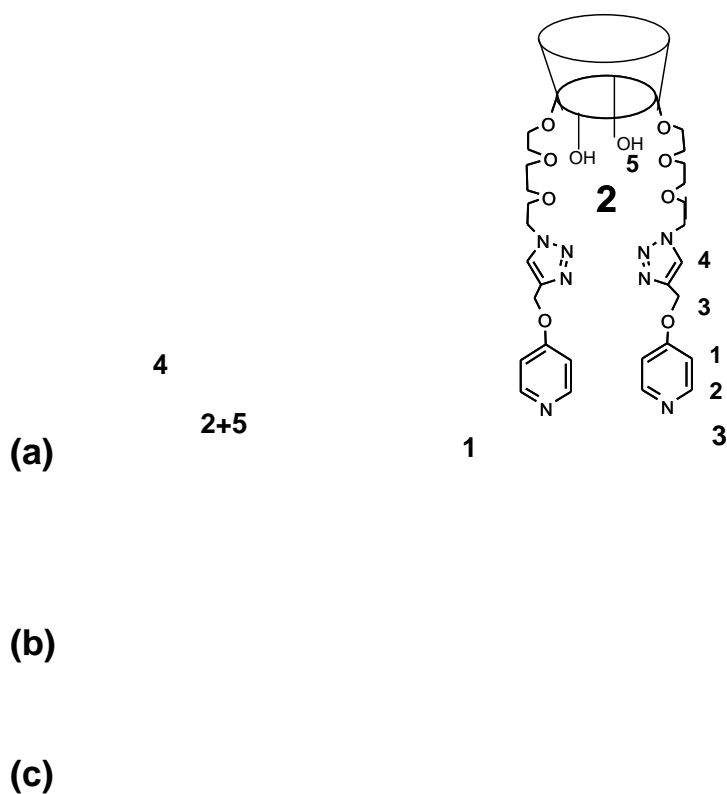
**Fig. S3** The MALDI-TOF mass spectrum of the **2**·Fe<sup>3+</sup> complex.



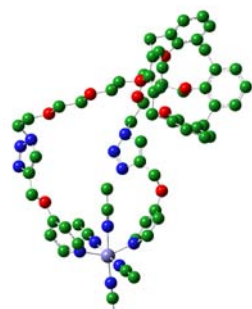
**Fig. S4** Photographs of the fluorescence responses (**2** (5×10<sup>-4</sup> M) in the absence and presence of 1.0 equiv Fe<sup>3+</sup> in CH<sub>3</sub>CN under UV light (λ<sub>ex</sub> = 254 nm).



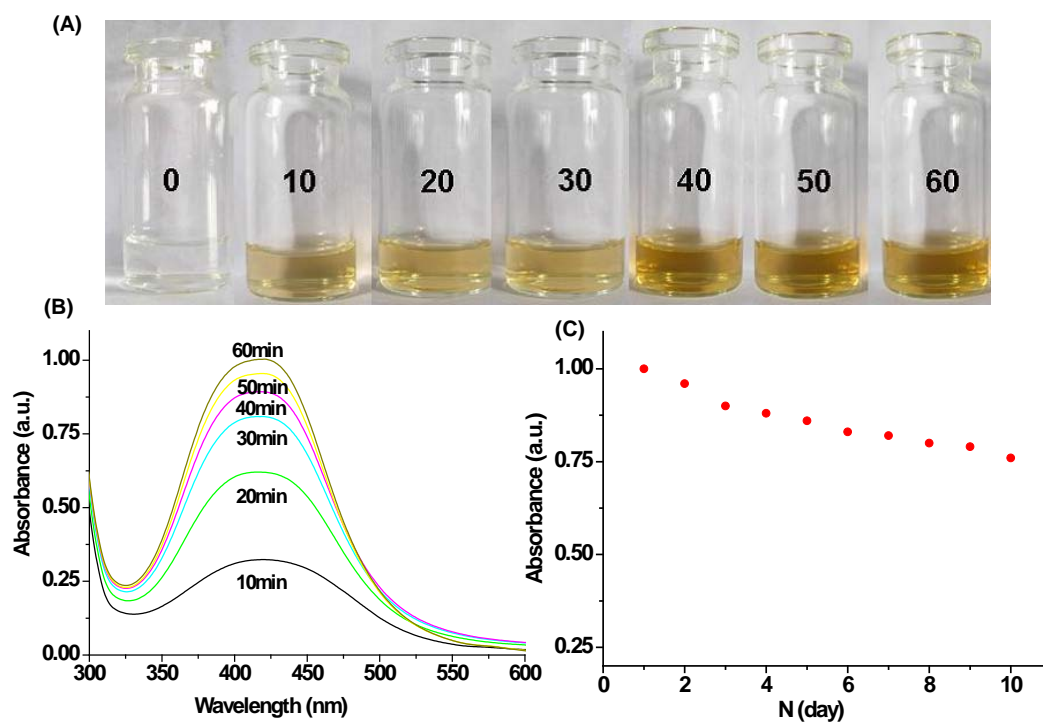
**Fig. S5.** The fluorescence changes of **2** ( $10^{-5}$  M) toward  $5.0 \times 10^{-5}$  M  $\text{Fe}^{3+}$  in the presence of  $1.0 \times 10^{-4}$  M other ions.  $I_0$  is fluorescence emission intensity at 313 nm for free **2**, and  $I$  is the fluorescent intensity upon addition of other metal ions with the existence of  $\text{Fe}^{3+}$ .



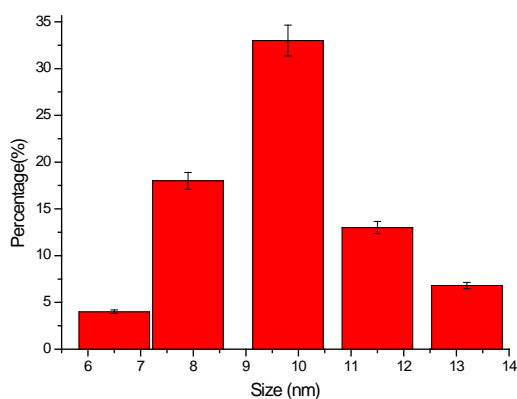
**Fig. S6.** The partial  $^1\text{H}$  NMR spectra of (c) **2** (5 mM) in  $\text{CD}_3\text{CN}$  and in the presence of (b) 1.0 equiv and (a) 2.0 equiv of  $\text{Fe}(\text{ClO}_4)_3$ .



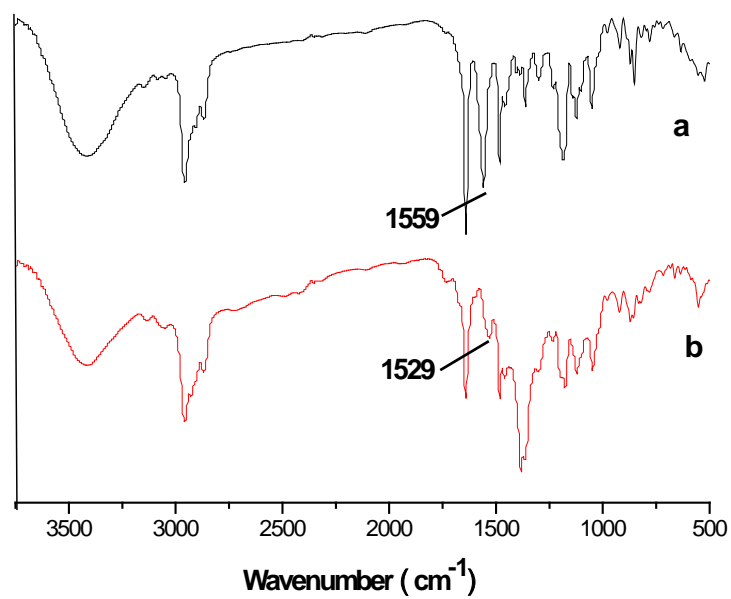
**Fig. S7.** The optimized structure of the  $2 \cdot \text{Fe}^{3+}$  complex



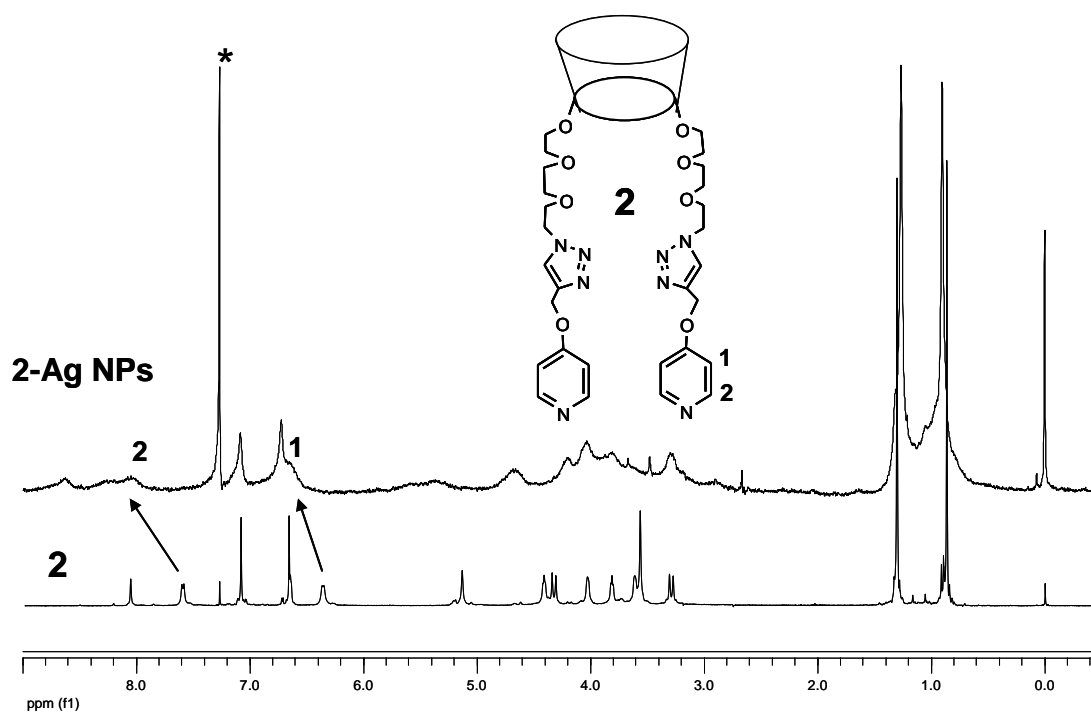
**Fig. S8.** The photographic images (A), UV-vis spectra (B) of  $2\text{-Ag}$  NPs on the increasing time (10-60 min) under the ultraviolet light at  $\lambda_{\text{max}} = 365\text{nm}$ . (C) The stability of the  $2\text{-Ag}$  NPs (the absorbance intensity at 414 nm).



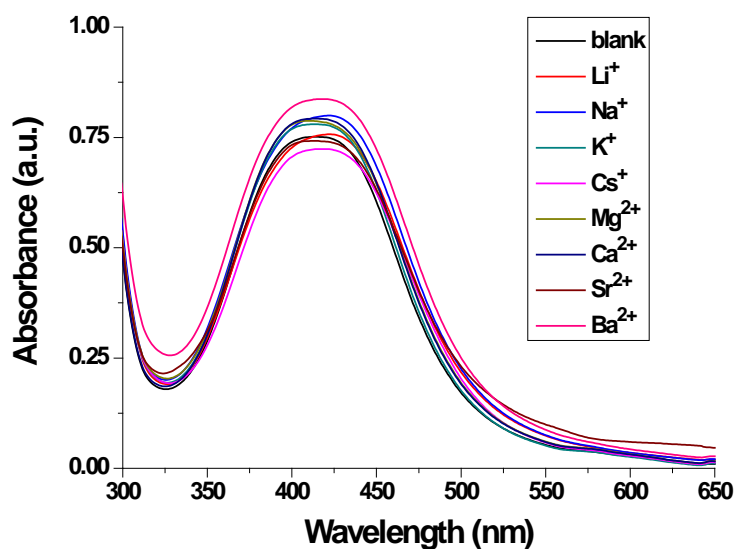
**Fig. S9** Size distribution of TEM images of  $2\text{-Ag}$  NPs.



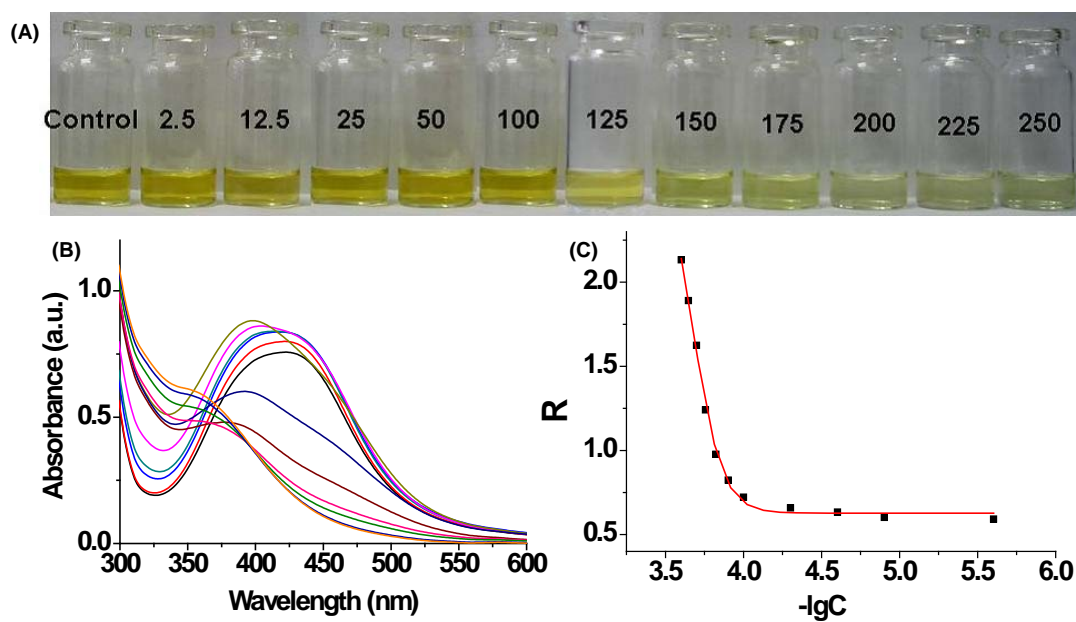
**Fig. S10** FT-IR spectra of (a) calix[4]arene **2** and (b) 2-Ag NPs



**Fig. S11**  $^1\text{H}$  NMR of calix[4]arene **2** and 2-Ag NPs in  $\text{CDCl}_3$ .

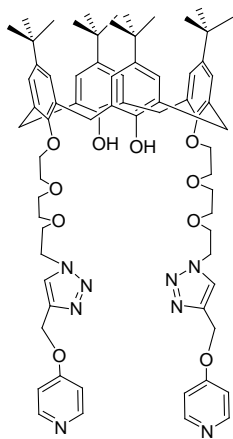
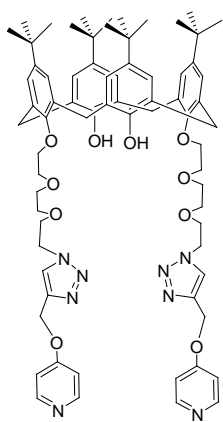


**Fig. S12** The UV-vis spectra of 2-Ag NPs, in the presence of different 0.2 mM alkali metal ions and alkaline earth metal ions (Li<sup>+</sup>, Na<sup>+</sup>, K<sup>+</sup>, Cs<sup>+</sup>, Mg<sup>2+</sup>, Ca<sup>2+</sup>, Sr<sup>2+</sup>, Ba<sup>2+</sup>) in methanol solutions.



**Fig. S13** The photographic images (A), UV-vis spectra (B) and the dependence of the R values (A<sub>364</sub>/A<sub>414</sub>) of (C) of 2-Ag NPs on the increasing concentration of Fe<sup>3+</sup> (2.5-250 μM). Typically, 0.5 mL of various concentrations of Fe<sup>3+</sup> were added into 1.5 mL 2-Ag NP solutions, and the combined solution mixed well for 30 min and then tested.





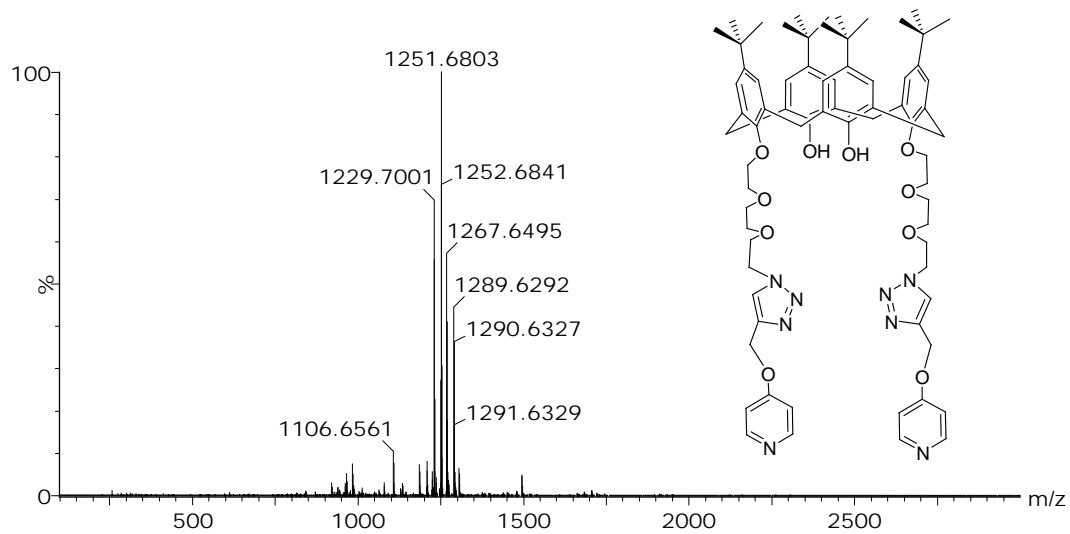


**Fig. S14** NMR and HDMS spectra of compounds **2**